Acta Technica *61*, No. 4B/2016, 19–28

Thermal oxidation kinetics analysis of ferrous sulfide under different heating rates[1]

Man Yang[2], Xianfeng Chen[2], Yujie Wang[2], Xiaoguang Yue[3]

Abstract. Ferrous sulfide (FeS) samples of the same mass were investigated by STA449F3 simultaneous thermal analyzer in order to analyze their thermal oxidation kinetics parameters. The reaction processes at different heating rates of 5 °C/min, 10 °C/min and 15 °C/min in air from 30 °C to 900 °C were comprehensively studied by thermogravimetry (TG), differential scanning calorimetry (DSC) and derivative thermogravimetry (DTG) methods. FeS kinetics parameters and reaction mechanism function were obtained with the combination of Satava-Sestak equation and Flynn–Wal–Ozawa (FWO) method. The results show that heating rates have significant effects on the characteristic temperatures of samples. With increase of heating rates, the characteristic temperatures of FeS samples gradually raise; the secondary reaction model acquired by the Satava–Sestak equation conforms to mechanism function; activation energy E obtained by FWO method is 153.83 kJ/mol, the pre-exponential factor A being $2.625 \cdot 10^8$.

Key words. Thermal oxidation kinetics, ferrous sulfide, mechanism function, characteristic temperatures, activation energy, pre-exponential factor..

1. Introduction

In storage and transportation of crude oil, active sulfur and organic sulfur in petroleum products together with the storage tank walls generate FeS. When FeS reacts with oxygen under some conditions coincident with exothermic reaction, continuous accumulation of heat can lead to high temperatures, even fire and explosion [1]. Meanwhile, oil tank fire and explosion seriously affect people's physical security and results in great losses in national economy [2–3].

Massive researches were made by many scholars for exploring the reasons of these accidents and thermal analysis kinetics was applied in the study of FeS ther-

[1]This work was supported by National Natural Science Foundation of China (projects No. 51374164, and No. 51174153).

[2]School of Resources and Environmental Engineering, Wuhan University of Technology, Wuhan 430070, China

[3]School of Civil Engineering, Wuhan University, Wuhan 430072, China

mal spontaneous mechanism in recent years [4–8]. The kinetic triplets [9], including activation energy A, pre-exponential factor E and mechanism function in differential form play an important role in evaluating energetic material stabilization in exothermic decomposition reaction. The activation energy regarded as the index of evaluating the spontaneous combustion tendency of FeS was usually calculated by the FWO, Kissinger, Coats–Redfern or Friedman method, respectively. To obtain the activation energy and mechanism function, the Iso-conversional method and Satava–Sestak equation were jointly applied in some references [10–12]. The activation energy and pre-exponential factor were acquired by the Iso-conversional methods, then the most probable mechanism function $f(\alpha)$ was inferred by combination with the Malek method [13]. However, the above methods could only obtain a part of the kinetic factors. Besides, according to our knowledge, there is no report regarding the application of a method to acquire FeS kinetic triplets in an easy and scalable way.

In this work, we report an easy way of obtaining activation energy, pre-exponential factor and mechanism at the same time, which is with the combination of Satava–Sestak equation and FWO method on the basis of TG, DSC and DTG analysis at different heating rates.

2. Experimental section

FeS ore (≥85.0 % purity) was purchased from Tianjin Guangfu Fine Chemical Co., Ltd. (Tianjin, China). Then it was dryed and dewatered in the electrothermal drying oven, grinded and screened after constant weight was attained, and finally, 200–240 mesh FeS samples were selected.

STA449F3 simultaneous thermal analyzer, produced by NETZSCH Company in Germany was purchased, where air was used as the purge gas with an air flow rate of 30 ml/min during the whole experiment. The samples with mass of 5 mg were measured at the heating rates of 5, 10 and 15 °C/min, respectively, from 30° to 900 °C.

Figures 1–3 shows the typical TG, DSC and DTG curves under different conditions. Generally for FeS, weight loss and weight gain phenomenon appear obviously with the increase of temperature from 30 °C to 300 °C. The initial weight loss could be ascribed to the removal of absorbed water, and weight gain indicated the absorption of oxygen. FeS exhibited a constant increase from 300 °C to 600 °C, which could be attributed to the weakening of physical absorption, slight beginning of chemisorption. The steep decrease in the weight of FeS at around 600 °C could be attributed to drastic combustion and release of SO_2. As shown in the Table 1, FeS ignition temperatures were 594, 615 and 628 °C under the heating rates of 5, 10 and 15 °C/min respectively. DSC curves (Fig. 1) had a small phase transformation absorption peak at around 140 °C. FeS had an obvious exothermic peak under the different heating rates. The initial temperatures of exothermic peaks were 570, 589 and 603 °C (Table 1), the corresponding peak temperatures were 620, 643 and 665 °C (Table 1). As shown in Fig. 3, although an obvious weight loss peak was presented under the different heating rates, the heating rates had less influence on

DTG curve. The maximum weight loss rate had slight increase, and the corresponding temperatures were 618, 646 and 665 °C (Table 1). TG, DSC and DTG curves all move to higher temperature direction with the increasing heating rate, which can be ascribed to the heat delivered from crucible to sample resulting in differential temperature between furnace and sample. Once temperature gradient occurred, the differential temperatures were also increasing with the heating rates.

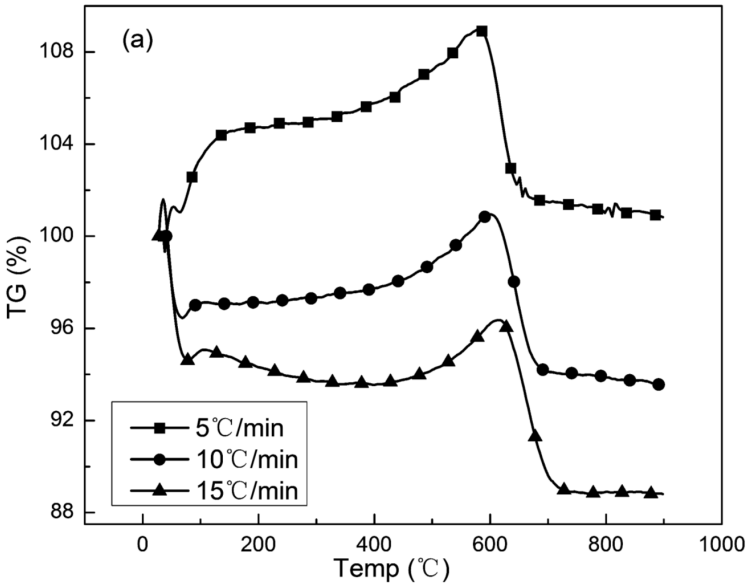

Fig. 1. TG curves of FeS under different heating rates

3. Theoretical analysis

The methods of thermal kinetics analysis [14, 15] can be classified as the application of thermal analysis techniques to study physical properties and chemical reaction rates and mechanism in materials, and to obtain the reaction dynamics parameters and mechanism functions. In order to determine the mechanism of solid state reaction and corresponding dynamics parameters, the study can start from the thermal kinetics equation.

FeS oxidation is a traditional gas-solid two-phase reaction, whose dynamics integration equation can be directly showed as follows

$$G(a) = \frac{A}{\beta} \int_0^T e^{-E/RT} \, \mathrm{d}T \,, \tag{1}$$

where α is the conversion degree, β is the heating rate (K/min), E is the activation energy (kJ/mol) A is the pre-exponential factor (K/s), $G(\alpha)$ is the integral expression

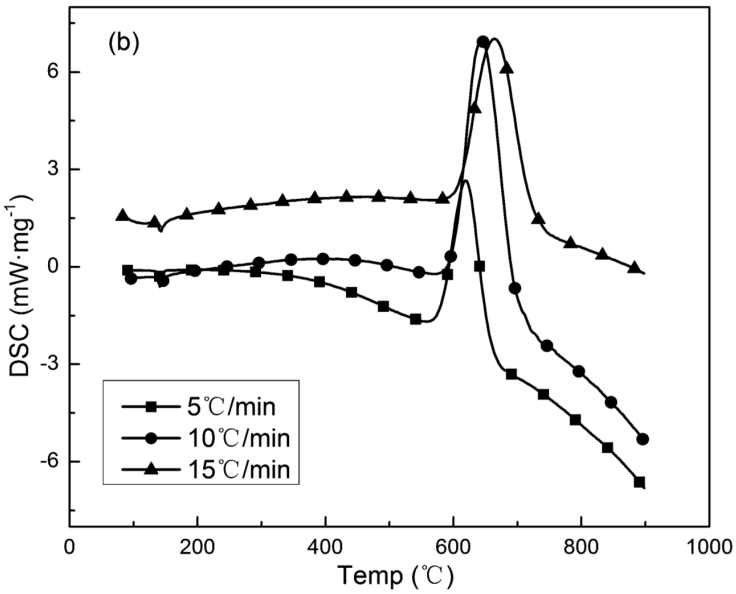

Fig. 2. DSC curves of FeS under different heating rates

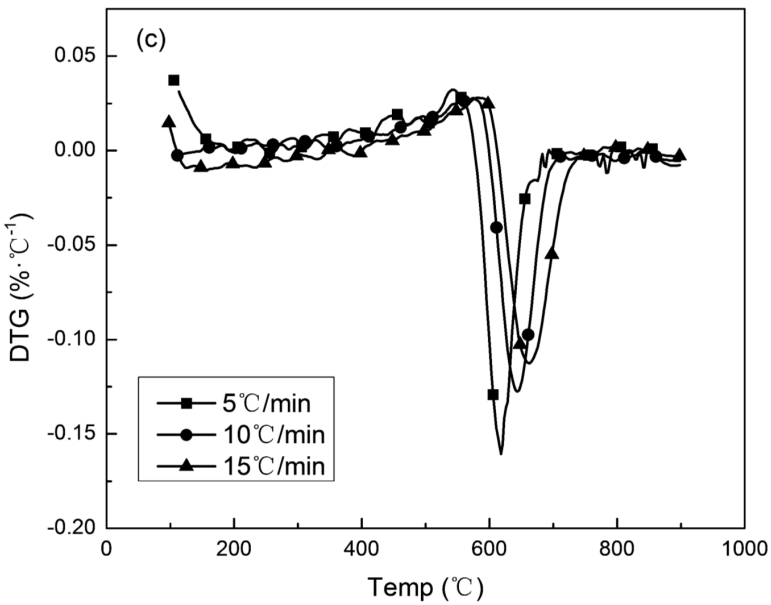

Fig. 3. DTG curves of FeS under different heating rates

of FeS oxidation reaction kinetics model, T is the reaction temperature, and R is the gas constant.

Table 1. Mode functions of commonly used gas solid reaction mechanism

Reaction mechanism	Symbol	Integral form $g(\alpha)$	Differential form $f(\alpha)$
One-dimensional diffusion	D1	α^2	$(2a)^{-1}$
Two-dimensional diffusion	D2	$\alpha + (1-\alpha)\ln(1-\alpha)$	$[-\ln(1-\alpha)]^{-1}$
Three-dimensional diffusion	D3	$\left[1-(1-\alpha)^{1/3}\right]^2$	$\frac{3}{2}(1-\alpha)\frac{2}{3}\left[1-(1-\alpha)^{1/3}\right]^{-1}$
Four-dimensional diffusion	D4	$(1-2a/3)-(1-a)^{2/3}$	$3/\left\{2\left[(1-a)^{-1/3}-1\right]\right\}$
Random nucleation theory and subsequent growth	A2	$[-\ln(1-a)]^{1/2}$	$2(1-a)\,[-\ln(1-a)]^{1/2}$
Random nucleation theory and subsequent growth	A3	$[-\ln(1-a)]^{1/3}$	$3(1-a)\,[-\ln(1-a)]^{2/3}$
Interface reaction	R1	α	1
Interface reaction	R2	$1-(1-\alpha)^{1/2}$	$2(1-\alpha)^{1/2}$
Interface reaction	R3	$1-(1-\alpha)^{1/3}$	$3(1-\alpha)^{2/3}$
First-order reaction	F1	$-\ln(1-\alpha)$	$1-\alpha$
Second order reaction	F2	$(1-\alpha)^{-1}-1$	$(1-\alpha)^2$

By integral transform of equation (1), FWO equation can be written as follows:

$$\lg\beta = \left[\frac{AE}{RG(\alpha)}\right] - 2.315 - 0.4567\frac{E}{RT} \tag{2}$$

With different β and the same α, $G\alpha$ is constant. Although FWO method is a common method to obtain the activation energy, E is directly obtained avoiding the problem of selecting suitable reaction mechanism functions, but the pre-exponential factor and reaction mechanism functions cannot be obtained.

After transformation of equation (1), Satava–Sestak equation can be attained in

the following form

$$\lg G(\alpha) = \left[\frac{A_{\mathrm{s}}E_{\mathrm{s}}}{R\beta}\right] - 2.315 - 0.4567\frac{E_{\mathrm{s}}}{RT}\,, \tag{3}$$

where A_{s} is a pre-exponential factor (in K/s) and E_{s} is the activation energy (kJ/mol). Both these quantities are obtained from the deformation of formula (2).

When β_i is fixed, T_{ij} and α_{ij} are substituted into the expression (3), then k equations can be expressed as follows

$$\lg G(\alpha_{ij}) = \left[\frac{A_{\mathrm{s}}E_{\mathrm{s}}}{R\beta_i}\right] - 2.315 - 0.4567\frac{E_{\mathrm{s}}}{RT_{ij}}\,, \tag{4}$$

where $i = \text{const}$ and $j = 1, 2, \ldots, k$. As β_i is fixed, then $\lg(A_sE_s/(R\beta_i)$ is a constant, thus the equation (4) is a linear equation and the linear least square method can be applied to solve these equations.

Substituting the mode functions (Table 1) into the equation (4) under different heating rates, and plotting $\lg G(\alpha)$ versus $1/T$ (see Figs. 4–6), one can obtain a series of curves, in which the best linear correlation curve represents FeS reaction mechanism.

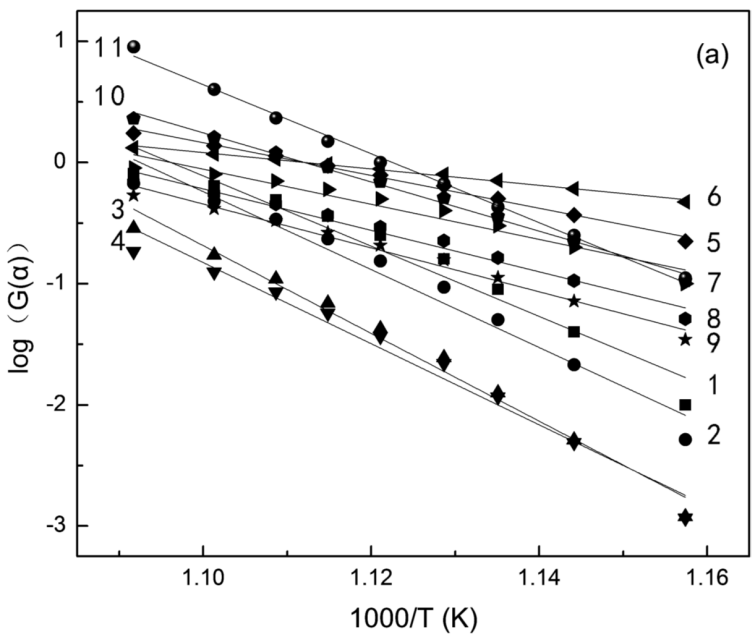

Fig. 4. Plots of $\lg G(\alpha)$ versus $1000/T$ at heating rate 5 °C/min: 1–D1, 2–D2, 3–D3, 4–D4, 5–A2, 6–A3, 7–R1, 8–R2, 9–R3, 10–F1, 11–F2

Then the determined reaction function of FeS is substituted into the expression (2), and after plotting $\lg G(\alpha)$ versus $1/T$, a curve can be obtained, and the

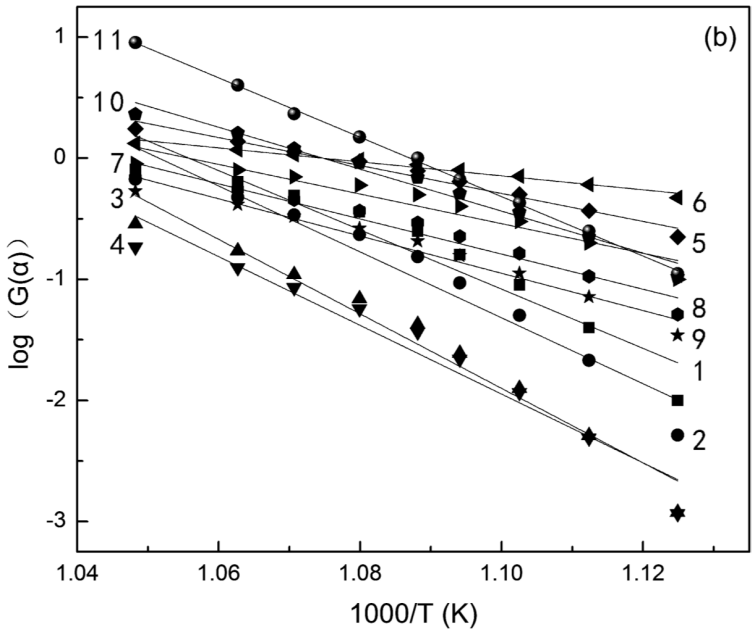

Fig. 5. Plots of $\lg G(\alpha)$ versus $1000/T$ at heating rate 10 °C/min: 1–D1, 2–D2, 3–D3, 4–D4, 5–A2, 6–A3, 7–R1, 8–R2, 9–R3, 10–F1, 11–F2

corresponding activation energy and pre-exponential factor of FeS with different conversion degrees can be calculated by slope intercept form.

Table 2. Correlation coefficients of various mechanism functions with temperature rate

Temperature rate (K/min)	5	10	15
D1	−0.9747	−0.956 89	−0.962 79
D2	−0.983 35	−0.968 38	−0.973 47
D3	−0.991 66	−0.980 32	−0.984 33
D4	−0.986 57	−0.972 85	−0.977 57
A2	−0.996 78	−0.988 85	−0.991 84
A3	−0.996 78	−0.988 85	−0.991 84
R1	−0.9747	−0.956 89	−0.962 79
R2	−0.988 18	−0.975 16	−0.979 67
R3	−0.991 66	−0.980 32	−0.984 33
F1	−0.996 78	−0.988 85	−0.991 84
F2	−0.997 91	−0.999 46	−0.999 54

Table 2 shows results of different kinds of functions substituted into equation (4) under different heating rates (5, 10 and 15 °C/min). It can be found that F2 mode has the best correlation, which can be taken as reaction mechanism function

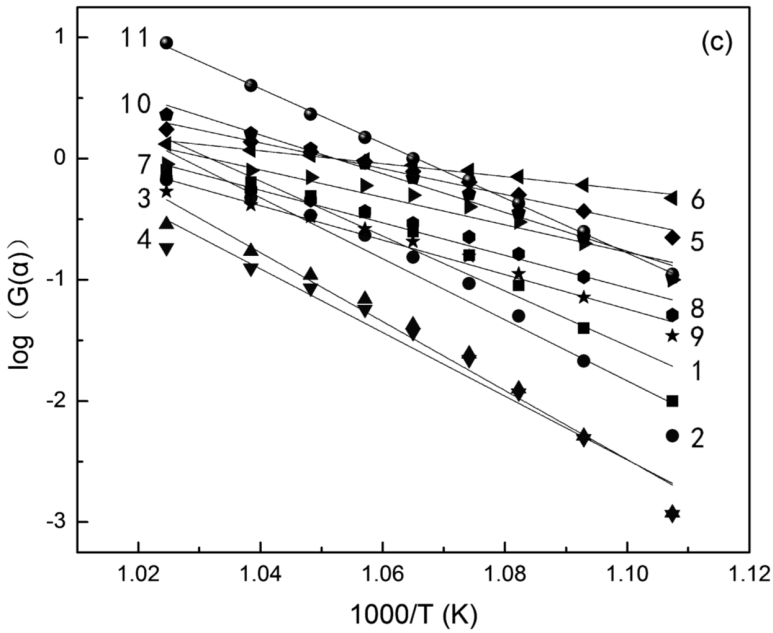

Fig. 6. Plots of $\lg G(\alpha)$ versus $1000/T$ at heating rate 15 °C/min: 1–D1, 2–D2, 3–D3, 4–D4, 5–A2, 6–A3, 7–R1, 8–R2, 9–R3, 10–F1, 11–F2

in the corresponding temperature interval. In other words, $G(\alpha) = (1-\alpha)^{-1}$, $f(\alpha) = (1-\alpha)^2$ represents the second order reaction. Besides, $E_{s5} = 167.46\,\mathrm{kJ/mol}$, $E_{s10} = 158.52\,\mathrm{kJ/mol}$ and $E_{s15} = 139.11\,\mathrm{kJ/mol}$.

Then substituting F2 mode into the expression (2), kinetic parameters can be obtained by the same conversion degree. The average conversion degree of each kinetic parameter is shown in Table 3, where the apparent activation energy $E_0 = 153.83\,\mathrm{kJ/mol}$ and $\lg A = 8.42$.

Table 3. Kinetic parameters of FeS conversion degree rate

α	E (kJ/mol)	A (K/s)	$R2$ (−)
0.1	173.071 920 9	552 981 875.2	0.998 97
0.2	169.692 617 6	586 904 014.2	0.999 73
0.3	164.805 616 7	423 117 732.1	0.999 43
0.4	159.133 637 3	264 105 090.2	0.999 98
0.5	155.570 286 4	212 791 055.6	0.995 01
0.6	150.960 540 2	150 989 879.3	0.998 22
0.7	143.791 057 8	79 637 006.5	0.999 99
0.8	138.437 293 3	59 113 532.42	0.999 27
0.9	128.998 254 5	32 468 236.13	0.999 27
average	153.829 025	262 456 491.3	

Finally

$$\left|\frac{E_0 - E_{\mathrm{s15}}}{E_0}\right| = 0.00957 < 0.1\,, \tag{5}$$

$$\left|\frac{E_0 - E_{\mathrm{s15}}}{E_0}\right| = 0.03049 < 0.1\,, \tag{6}$$

$$\left|\frac{E_0 - E_{\mathrm{s15}}}{E_0}\right| = 0.0886 < 0.1\,. \tag{7}$$

According the above criterion, the results of expressions (5), (6) and (7) are smaller than 0.1, thus FeS thermo-oxidation is in accordance with the secondary reaction model (F2): integral form $G(\alpha) = (1-\alpha)^{-1}$, the corresponding activation energy E is 153.83 kJ/mol, and the pre-exponential factor is $A = 2.625 \times 10^8$.

4. Conclusion

- According to the TG, DSC and DTG curves, the heating rates have significant effects on the peak temperatures of samples. Under the heating rate of 5, 10 and 15 °C/min, respectively, FeS ignition temperatures were 594, 615 and 628 °C, the initial temperatures of exothermic peak were 570, 589 and 603 °C, the corresponding peak temperatures were 620, 643 and 665 °C, the corresponding temperatures of the maximum weight loss rate were 618, 646 and 665 °C. The results show that the characteristic temperatures of FeS samples will gradually raise with the increase of heating rate.

- FeS dynamic parameters and reaction mechanism functions of thermo-oxidation were solved with combination of Satava–Sestak method and FWO method. FeS thermo-oxidation determined by Satava–Sestak equation is in accordance with the secondary reaction model (F2): integral form $G(\alpha) = (1-\alpha)^{-1}$, activation energy E of FeS thermo-oxidation obtained by FWO method is 153.83 kJ/mol and the pre-exponential factor $A = 2.625 \times 10^8$.

References

[1] Z. H. Zhang, S. L. Zhao, P. Li, Y. Han: *Spontaneous combustion process of hydrogen sulfide corrosion products formed at room temperature.* Acta Petrolei Sinica (Petroleum Processing Section) *28* (2012), No. 1, 122–126.

[2] S. Lei, S. Jian, X. Kui: *Fuzzy fault tree assessment based on improved AHP for fire and explosion accidents for steel oil storage tanks.* J Hazardous Materials *278* (2014), 529–538.

[3] D. Y. Zhang, A. Z. Ding, S. C. Cui, C. Hu, S. F. Thornton, J. Dou, Y. Sun, W. E. Huang: *Whole cell bioreporter application for rapid detection and evaluation of crude oil spill in seawater caused by Dalian oil tank explosion.* Water Research *47* (2013), No. 3, 1191–1200.

[4] S. R. Niranjan, N. Datta, K. Suresh: *Effect of Fe modification on H_2S sensing properties of rheotaxially grown and thermally oxidized SnO_2 thin films.* Mat. Chem. Phys. *156* (2015), 227–237.

[5] N. Y. Dzade, A. Roldan, N. H. de Leeuw: *Adsorption of methylamine on mackinawite (FeS) surfaces: A density functional theory study.* J Chem. Phys. *139* (2013), No. 12, 28–36.

[6] W. H. Wang, Z. S. Xu, B. J. Sun, D. Liang: *Experiment investigation on spontaneous combustion of iron sulfides in oil tank.* Advanced Materials Research *750–752* (2013), 1758–1764.

[7] F. Q. Yang, C. Wu, H. Liu, W. Pan, Y. Cui: *Thermal analysis kinetics of sulfide ores for spontaneous combustion.* J Central South University (Science and Technology) *42* (2011), No. 8, 2469–2474.

[8] M. J. Glenn, J. A. Allen, S. W. Donne: *Thermal investigation of a doped alkali-metal carbonate ternary eutectic for direct carbon fuel cell applications.* Energy & Fuels *29* (2015), No. 8, 5423–5433.

[9] M. Malow, U. Krause: *The overall activation energy of the exothermic reactions of thermally unstable materials.* J Loss Prevention in the Process Industries *17* (2004), No. 1, 51–58.

[10] M. Yang, X. F. Chen, Y. J. Shang, R. D. Bao: *Particle size effect on FeS spontaneous combustion characters in petroleum.* Appl. Mech. Mater. *608–609*, (2014), 971 to 975.

[11] S. P. Zhao, J. C. Jiang, Y. X. Yang: *Thermal kinetic analysis on oxidation of FeS based on thermal gravimetric experiments.* Acta Petrolei Sinica (Petroleum Processing Section) *26* (2010), No. 6, 972–976.

[12] Huang Lei, Chen Yucheng, Liu Geng, Li Shengnan, Liu Yun, Gao Xu: *Non-isothermal pyrolysis characteristics of giant reed (Arundo donax L.) using thermogravimetric analysis.* Energy *87* (2015), 31–40.

[13] J. Z. Liang, J. Z. Wang, G. C. P. Tsui, C, Y. Tang: *Thermal decomposition kinetics of polypropylene composites filled with graphene nanoplatelets.* Polymer Testing *48* (2015), 97–103.

[14] M. Montazeri-Gh, M. Mahmoodi-k: *Optimized predictive energy management of plug-in hybrid electric vehicle based on traffic condition.* J Cleaner Production *149* (2016), 935–948.

[15] A. N. D'yachenko, R. I. Kraidenko: *Processing oxide-sulfide copper ores using ammonium chloride.* Russian Journal on Non-ferrous Metals *51* (2010), No. 5, 377–381.

Received November 16, 2016